BNL-230134-2026-TECH

CA/AP/758

On the Recombination of High Energy Hadrons with Electrons

G. Wang

August 2026

Collider Accelerator Department

Brookhaven National Laboratory

U.S. Department of Energy

USDOE Office of Science (SC), Nuclear Physics (NP)

DISCLAIMER

On the Recombination of High Energy Hadrons with Electrons

Gang Wang, [1,2,*] Dmitry Kayran,[1,2] Nikhil Bachhawat, [2] Yichao Jing,[1,2] Vladimir N. Litvinenko, [2,1] Jun Ma[1,2] and Igor Pinayev[1]

[1]Collider-Accelerator Department, Brookhaven National Laboratory, Upton, New York 11973-5000, USA
[2]Department of Physics and Astronomy, Stony Brook University, New York 11794, USA

For a system with the ion beam co-propagating with the electron beam, such as a traditional electron cooler or a Coherent electron Cooler (CeC), the recombination rate is an important observable for matching the energy of the electrons with that of the ions [1, 2]. In this work, we have developed analytical expressions to calculate how the recombination rate depends on the energy difference of the two beams, with the influences from the transverse motions of the particles being considered. The analytical results are then applied to analyze the measured recombination data collected during the CeC experiment.

I. INTRODUCTION.

The CeC experiment at RHIC targets cooling Au^{+79} ions with electrons at the energy of γ = 28.5 [3] for Run 21-22 and at the energy of γ = 19.6 for Run 25. One of the major challenges in the experiment is to ensure that the electron beam has the same energy as that of the ion beam. A common technique used for the energy matching is by measuring the recombination rate. Since the recombination rate is maximized when the velocities of the two beams coincide, the optimal energy of the electrons can be identified by scanning the energy of the electrons while monitoring the recombination rate. How fast the recombination rate decreases with the energy deviation from the optimal energy depends on the 3D velocity spread of the electrons and the ions. During RHIC run 21, it was found in the CeC experiment that the measured recombination rate drops much slower than what one would expect solely from the measured energy spread of the electrons and the ions. One of the major candidates responsible for the discrepancy is the transverse motion of the particles which had been neglected from the analytical estimates. In this work, we have derived analytical expressions to calculate the recombination rate with transverse motion of the particles taken into account. The analytical results are then used to fit the data collected during the CeC experiment. Since the angular spreads of the electrons and ions can be calculated from the measured emittances and beta function, the parameter to be determined from fitting the measured recombination data is the orbital misalignment of the electron bunch with respect to that of the ion bunch. The orbital angle obtained from fitting the recombination data clearly shows the improvement of the orbit alignment in run 25 as a result of the beam based alignment performed after run 22.

In section II, we show the analytical formula derived to calculate the recombination rate for various velocity distributions of the electrons and the ions. A description of the experiment setup is given in Section III. Section IV consists of the results from analyzing the experiment data collected during the RHIC runs and a short summary is given in section V.

II. Calculation of the Recombination Rate

For an electron bunch co-propagating with an ion bunch in an electron cooler, the recombination rate is calculated from the following equation:

$$R = \gamma^{-2} N_{ion} N_{bunch} \frac{\sigma_{es}}{\sigma_{is}} n_e \frac{L_{cool}}{L_{ring}} \alpha_r , \qquad (1)$$

where γ is the Lorentz factor describing the energy of the two beams, N_{ion} is the number of ions in the ion bunch, N_{bunch} is the number of electron bunches overlapping with an ion bunch, σ_{es} is the R.M.S. bunch length of the electron bunch, σ_{is} is the R.M.S. bunch length of the ion bunch, n_e is the spatial density of the electrons, L_{cool} is the length of the cooling section, L_{ring} is the circumference of the ion storage ring and α_r is the recombination rate coefficient. The recombination rate coefficient is given by the following integral over the velocity distribution of the electrons and the ions [2]

$$\alpha_r = \frac{\int_{-\infty}^{\infty} d^3v_i d^3v_e f_e(v_e) f_I(v_i) \left|\vec{v}_e - \vec{v}_i\right| \sigma\left(\left|\vec{v}_e - \vec{v}_i\right|\right)}{\int_{-\infty}^{\infty} d^3v_i d^3v_e f_e(v_e) f_I(v_i)} \qquad (2)$$

* gawang@bnl.gov

where

$$\sigma(v) = A\frac{2h\nu_0}{m_e v^2}\left[\ln\left(\sqrt{\frac{2h\nu_0}{m_e v^2}}\right)+\gamma_1+\gamma_2\left(\frac{m_e v^2}{2h\nu_0}\right)^{1/3}\right] \quad (3)$$

is the recombination cross section which depends on the relative velocity of an ion with respect to an electron, and $f_e(v_e)$ and $f_I(v_i)$ are the velocity distributions of the electrons and the ions. The constants in eq. (3) are $A=2.11\times10^{-22}cm^2$, $\gamma_1=0.1402$ and $\gamma_2=0.525$. The binding energy of an electron in the ground state of the ion is given by

$$h\nu_0 = Z^2\alpha^2 m_e c^2/2 = Z^2\times13.6eV,$$

where Z is the charge number of the ion, α is the fine structure constant and m_e is the mass of an electron.

A. Velocity Distribution

The velocity distribution of the electrons and the ions can be sufficiently approximated by the following expression:

$$f_e(v_e) = \frac{1}{(2\pi)^{3/2}\beta_{e,x}\beta_{e,y}\beta_{e,z}} \exp\left(-\frac{(v_{e,x}-v_{0,x})^2}{2\beta_{e,x}^2}-\frac{(v_{e,y}-v_{0,y})^2}{2\beta_{e,y}^2}-\frac{(v_{e,z}-v_{0,z})^2}{2\beta_{e,z}^2}\right), \quad (4)$$

and

$$f_i(v_i) = \frac{1}{(2\pi)^{3/2}\beta_{i,x}\beta_{i,y}\beta_{i,z}}\exp\left(-\frac{v_{i,x}{}^2}{2\beta_{i,x}^2}-\frac{v_{i,y}{}^2}{2\beta_{i,y}^2}-\frac{v_{i,z}{}^2}{2\beta_{i,z}^2}\right) \quad (5)$$

where $\beta_{e,j}$ and $\beta_{i,j}$ (for $j=x,y,z$) are velocity spreads of the electrons and the ions in the co-moving frame. Eq. (4) also includes an average velocity deviation, $\vec{v}_0$, of the electrons with respect to the ions, which can be introduced by an orbital angle of the electrons in the transverse direction and an energy mismatch of the electrons in the longitudinal direction.

B. Isotropic Transverse Velocity Distribution

In most electron coolers, the transverse velocity spreads of the electrons and the ions are isotropic, i.e. their horizontal velocity spread equal to their vertical velocity spread. Consequently, we can assume that the velocity distribution of the electrons is

$$f_e(v_e) = \frac{1}{2\pi\beta_{e,\perp}^2}\exp\left(-\frac{(v_{e,x}-v_{x0})^2+v_{e,y}^2}{2\beta_{e,\perp}^2}\right)f_{e,z}(v_{e,z}) \quad (6)$$

and that of the ions is

$$f_I(v_i) = \frac{1}{2\pi\beta_{i,\perp}^2}\exp\left(-\frac{v_{i,x}^2+v_{i,y}^2}{2\beta_{i,\perp}^2}\right)f_{i,z}(v_{i,z}), \quad (7)$$

with $\beta_{e,\perp}$ and $\beta_{i,\perp}$ being the transverse velocity spreads of the electrons and the ions. For simplicity, we assume that the transverse velocity of the electron bunch is in the horizontal plane and hence $v_{0,y}=0$. Inserting eq. (6) and eq. (7) into eq. (2) yields

$$\alpha_r = \frac{\int_{-\infty}^{\infty} d^3v v\sigma(v) \mathrm{e}^{-m_e\left((v_x-v_{0,x})^2+v_y{}^2\right)/2kT_{ei}} \int_{-\infty}^{\infty} f_{e,z}(v_z+v_{i,z})f_{i,z}(v_{i,z})dv_{i,z}}{(2\pi kT_{ei}/m_e)\int_{-\infty}^{\infty} f_{e,z}(v_z+v_{i,z})f_{i,z}(v_{i,z})dv_z dv_{i,z}}, \quad (8)$$

where we defined the effective temperature parameter

$$T_{ei} = \frac{m_e}{k}\left(\beta_{e,\perp}^2+\beta_{i,\perp}^2\right). \quad (9)$$

1. Longitudinally Cold Electrons and Ions

Typically, the longitudinal velocity spread in the beam frame is much smaller than the transverse velocity spread and hence we can take the delta function for the longitudinal velocity distribution, i.e. $f_{e,z}(v_{e,z})=\delta(v_{e,z}-v_{z0})$ and $f_{i,z}(v_{i,z})=\delta(v_{i,z})$. In this case, eq. (8) becomes

$$\alpha_r = \frac{1}{2\pi kT_{ei}/m_e}\int_{-\infty}^{\infty} d^3v v\sigma(v) \times \mathrm{e}^{-m_e\left((v_x-v_{0,x})^2+v_y{}^2\right)/2kT_{ei}}\delta(v_z-v_{0,z}). \quad (10)$$

The recombination cross section for an electron moving with velocity $\vec{v}$ with respect to the ion is [2]

$$\sigma(v) = A\frac{2h\nu_0}{m_e v^2}\left[\ln\left(\sqrt{\frac{2h\nu_0}{m_e v^2}}\right)+\gamma_1+\gamma_2\left(\frac{m_e v^2}{2h\nu_0}\right)^{1/3}\right], \quad (11)$$

where $A=2.11\times10^{-22}cm^2$, $h\nu_0=Z^2\times13.6eV$, Z is the charge number of the ion, $\gamma_1=0.1402$ and $\gamma_2=0.525$. Inserting eq. (11) into eq. (10) yields

$$\alpha_r = \frac{Ach\nu_0}{kT_{ei}}\sqrt{\frac{2h\nu_0}{m_e c^2}}\mathrm{e}^{m_e\left(v_{0,z}^2-v_{0,x}^2\right)/(2kT_{ei})}\int_{\frac{m_e v_{0,z}^2}{2h\nu_0}}^{\infty}\frac{\mathrm{e}^{-h\nu_0 y/(kT_{ei})}}{\sqrt{y}}\times \left(\gamma_1+\gamma_2 y^{1/3}-\frac{1}{2}\ln y\right)I_0\left(\frac{v_{0,x}\sqrt{2m_e h\nu_0}}{kT_{ei}}\sqrt{y-\frac{m_e v_{0,z}^2}{2h\nu_0}}\right)dy. \quad (12)$$

where $I_0(x)$ is the modified Bessel function.

2. Longitudinally Warm Electrons and Ions

If the longitudinal velocity spread is not negligible, the longitudinal velocity distribution becomes

$$f_{e,z}(v_{e,z}) = \frac{1}{\sqrt{2\pi}\beta_{e,z}}\exp\left(-\frac{(v_{e,z}-v_{0,z})^2}{2\beta_{e,z}^2}\right), \quad (13)$$

* gawang@bnl.gov

and

$$f_{i,z}\left(v_{i,z}\right)=\frac{1}{\sqrt{2\pi}\beta_{i,z}}\exp\left(-\frac{v_{i,z}{}^{2}}{2\beta_{i,z}^{2}}\right). \quad (14)$$

Inserting eq. (13) and (14) into eq. (8) yields

$$\alpha_r = Ac\frac{4\left(h\nu_0\right)^2}{\pi^{1/2}kT_{ei}\sqrt{kT_z\cdot m_e c^2}}\exp\left(\frac{-m_e v_{0,z}^2}{4kT_z}-\frac{m_e v_{0,x}^2}{2kT_{ei}}\right),$$
$$\times\int_0^\infty y\left[-\ln\left(y\right)+\gamma_1+\gamma_2 y^{2/3}\right]\exp\left(-\frac{h\nu_0}{kT_{ei}}y^2\right)I\left(y\right)dy \quad (15)$$

with

$$I\left(y\right)=\int_0^1\exp\left(-\frac{h\nu_0}{2kT_z}y^2\left(1-\frac{2T_z}{T_{ei}}\right)x^2\right), \quad (16)$$
$$\times\cosh\left(\frac{\sqrt{2m_e h\nu_0}v_{0,z}}{2kT_z}yx\right)I_0\left(\frac{v_{0,x}\sqrt{2m_e h\nu_0}}{kT_{ei}}y\sqrt{1-x^2}\right)dx$$

and

$$T_z=\frac{m_e}{2k}\left(\beta_{e,z}^2+\beta_{i,z}^2\right). \quad (17)$$

In the absence of the transverse orbital angle, i.e. $v_{0,x}=0$, eq. (15) can be simplified to the following 1D integral,

$$\alpha_r=\frac{Ach\nu_0}{kT_{ei}\eta}\sqrt{\frac{2h\nu_0}{m_e c^2}}\,\mathrm{e}^{\frac{m_e v_{0,z}{}^2\left(1-\eta^2\right)}{4kT_z\eta^2}}\int_0^\infty\left(\gamma_1+\gamma_2 y^{2/3}-\ln y\right)$$
$$\times\mathrm{e}^{-\frac{h\nu_0 y^2}{kT_{ei}}}\left\{erf\left[\eta\sqrt{\frac{h\nu_0}{2kT_z}}\left(y+\sqrt{\frac{m_e}{2h\nu_0}}\frac{v_{0,z}}{\eta^2}\right)\right]\right., \quad (18)$$
$$\left.+erf\left[\eta\sqrt{\frac{h\nu_0}{2kT_z}}\left(y-\frac{v_{0,z}}{\eta^2}\sqrt{\frac{m_e}{2h\nu_0}}\right)\right]\right\}dy$$

where $\eta=\sqrt{1-2T_z/T_{ei}}$. It is worth noting that for $T_{ei}<2T_z$, η is imaginary but according to the relation, $erf\left(i\cdot x\right)=i\cdot erfi\left(x\right)$, the error function in eq. (18) also returns an imaginary value and hence the expression is real and still valid for calculating the recombination rate. Eq. (18) has a singularity at $T_{ei}=2T_z$ and in this case, the following expression can be used

$$\alpha_r=\frac{Ah\nu_0}{m_e v_{z0}}\sqrt{\frac{2h\nu_0}{\pi kT_z}}\,\mathrm{e}^{\frac{-m_e v_{z0}{}^2}{4kT_z}}. \quad (19)$$
$$\times\int_0^\infty\frac{\gamma_1+\gamma_2 y^{1/3}-\frac{1}{2}\ln y}{\sqrt{y}}\mathrm{e}^{-\frac{h\nu_0 y}{2kT_z}}\sin h\left(\frac{v_{z0}\sqrt{m_e h\nu_0 y}}{\sqrt{2}kT_z}\right)dy$$

C. Anisotropic Transverse Velocity Distribution

If the transverse velocity spread in the horizontal plane and that in the vertical plane are different, eq. (6) and eq. (7) becomes

$$f_e\left(v_e\right)=\frac{1}{2\pi\beta_{e,x}\beta_{e,y}}\exp\left(-\frac{v_{e,x}^2}{2\beta_{e,x}^2}-\frac{v_{e,y}^2}{2\beta_{e,y}^2}\right)f_{e,z}\left(v_{e,z}\right) \quad (20)$$

and

$$f_I\left(v_i\right)=\frac{1}{2\pi\beta_{i,x}\beta_{i,y}}\exp\left(-\frac{v_{i,x}^2}{2\beta_{i,x}^2}-\frac{v_{i,y}^2}{2\beta_{i,y}^2}\right)f_{i,z}\left(v_{i,z}\right). \quad (21)$$

We further assume that the longitudinal velocity spreads of the electrons and that of the ions in the co-moving frame are significantly smaller than the transvers velocity spread and can be treated as cold beam, i.e.

$$f_{e,z}\left(v_{e,z}\right)=\delta\left(v_{e,z}-v_{z0}\right), \quad (22)$$

and

$$f_{i,z}\left(v_{i,z}\right)=\delta\left(v_{i,z}\right). \quad (23)$$

Inserting eq. (20)-(23) into eq. (2) and carrying out the integration yields

$$\alpha_r=\frac{Ach\nu_0}{m_e\beta_x\beta_y}\sqrt{\frac{2h\nu_0}{m_e c^2}}\int_0^\infty\frac{dy}{\sqrt{y+\frac{m_e v_{z0}^2}{2h\nu_0}}}\exp\left(-\frac{h\nu_0}{kT_1}y\right), \quad (24)$$
$$I_0\left(\frac{h\nu_0}{kT_1}\eta\cdot y\right)\left[-\frac{1}{2}\ln\left(y+\frac{m_e v_{z0}^2}{2h\nu_0}\right)+\gamma_1+\gamma_2\left(y+\frac{m_e v_{z0}^2}{2h\nu_0}\right)^{1/3}\right]$$

where

$$kT_1\equiv\frac{2m_e\beta_x^2\beta_y^2}{\beta_x^2+\beta_y^2}, \quad (25)$$

$$\eta\equiv\frac{\beta_x^2-\beta_y^2}{\beta_x^2+\beta_y^2}, \quad (26)$$

$$\beta_x\equiv\sqrt{\beta_{i,x}^2+\beta_{e,x}^2}, \quad (27)$$

and

$$\beta_y\equiv\sqrt{\beta_{i,y}^2+\beta_{e,y}^2}. \quad (28)$$

III. EXPERIMENT SETUP

The measurement of the recombination signal has been performed during the CeC experiment. As shown in fig. 1, the electron beam is generated in the 112 MHz SRF gun and ballistically compressed to the desired bunch length through the 500 MHz normal conducting bunching cavity. A 5-cell SRF linac is used to accelerate the electron beam to 14 MeV and a dogleg transfer beam line is used to bring the electron beam to the cooling section where it merges with the circulating ion beam in the yellow ring of RHIC. A scintillator is installed downstream of the cooling section to capture the recombined ions, and the number of captured ions is the recombination signal used for the energy alignment of the electron beam and the ion beam. An orbit bump is set up for the ion beam

* gawang@bnl.gov

at the location of the scintillator to increase the strength of the recombination signal.

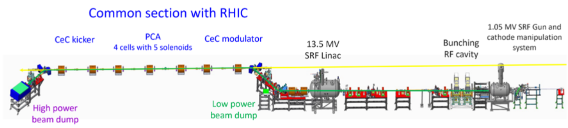

FIG 1: Schematic layout of the CeC experiment.

The initial measurement of the recombination signal was performed during RHIC Run 21 and Run 22. The parameters of the CeC experiment for Run 21 and Run 22 are listed in Table 1.

Table 1: Parameters of the CeC experiment at RHIC for Run 21 and Run 22

	Electrons	**Ions**
Energy, γ	28.5	
Energy spread R.M.S.	5E-4	1.3E-3
Angular spread, mrad	0.3	0.14

The measurement was resumed during RHIC Run 25 with a new beam energy, as shown in table 2. Compared with the parameters in the previous runs, the emittance and the energy spread of the electron beam have been significantly reduced as a result of smaller bunch charge and better controls of the orbit and optics.

Table 2: Parameters of the CeC experiment at RHIC for Run 25

	Electrons	**Ions**
Energy, γ	19.6	
Energy spread R.M.S.	2E-4	1.23 E-3
Angular spread, mrad	0.18	0.16

IV. EXPERIMENT RESULT

During RHIC run 21 and 22, the electrons were brought to co-propagate with the ions in the 14 meters long cooling section and the recombination rate were measured while scanning the energy of the electrons. As shown in table 1, the designed angular spread at cooling section is about 0.3 mrad for the electrons and 0.14 mrad for the ions, which corresponds to the transverse temperature of the particles in the comoving frame of $kT_{ei} = 46.7eV$. Fig. 1 (red triangles) shows the normalized recombination rate as a function of the electrons' energy as measured in run 21 (Left) and run 22 (Right). The energy of the electrons was adjusted by changing the voltage of the accelerating cavities. As shown in fig. 2 (solid blue curve), eq. (12) provides reasonable fit for the measured data if we assume that there was an orbital angle between the electrons and the ions with the value of 0.77 mrad for the run 21 measurement and 0.7 mrad for the run 22 measurement. The alignment of the electron beam and the ion beam in the cooling section are achieved with beam position monitors (BPMs), earth field compensation coils and dipole correctors. During the measurements, the beam position readings at the BPMs were within $\pm 1\ mm$ and the distances between two successive BPMs are 1~2 meters. Consequently, we consider it reasonable to assume an angular misalignment in the level of 0.7~0.8 mrad which was responsible for the slow declining in the recombination rate with the energy deviation of the electron beam.

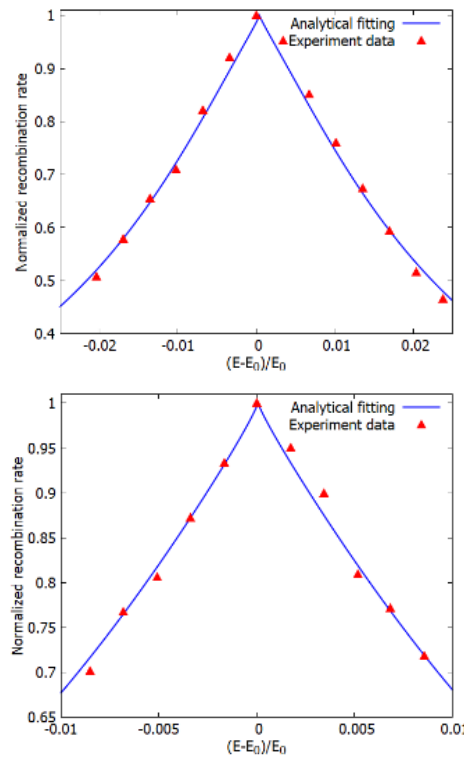

FIG 2. Normalized recombination rate as a function of the relative energy deviation of the electron bunch. (Top) The data were taken during RHIC run 21. The red triangles represent the measured recombination rate normalized to the value at $E_0 = 14.72MeV$ and the blue curve represents the fitting from eq. (12) with $v_{x0} = 6.6\times10^6 m/s$, which corresponds to 0.77 mrad of orbital angle between the electron beam and the ion beam. (Bottom) The data were taken during RHIC run 22. The measured recombination rate maximizes at $E_0 = 14.65MeV$ and the fitting curve were calculated with $v_{x0} = 6\times10^6 m/s$, i.e. 0.7 mrad of orbital angle between the two beams.

* gawang@bnl.gov

In 2025, the CeC experiment changed the beam energy and electron bunch charge, which leads to smaller emittance and hence angular spread in the cooling section. Consequently, the longitudinal velocity spread in the cooling section may not be neglected and eq. (15) should be used to calculate the recombination rate for a longitudinally warm electron beam. Fig. 3 shows the measured recombination signal as a function of the relative energy deviation of the electrons with respect to that of the ions. Since the detector only captures a small portion of the recombined ions, the measured signal (blue triangles) was significantly lower than what was expected from the calculation. The red curve in fig. 3 was created by multiplying the recombination rate as calculated from eq. (15) by 0.046 and it shows that if we assume only 4.6% of the recombined ions were captured by the detector, the orbital angle in the cooling section between the two beams is 0.42 mrad. Compared with the orbital angle measured during Run 21 and Run 22, the alignment of the orbits of the electron and ion beam was improved by 50% in Run 25, which is to be expected from the beam-based alignment performed in Run 24 and Run 25.

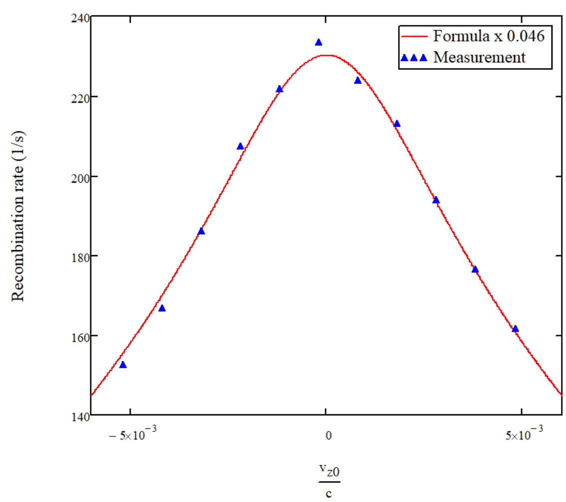

FIG 3. Measured recombination signal as a function of the relative energy deviation of the electrons w.r.t. that of the ions. The blue triangles are the measured data and the red solid curve is the recombination rate as calculated from eq. (15) multiplied by a factor of 0.046. Since only partial of the recombined ions are captured by the detector, the measured recombination rate is always smaller than the calculated rate. By comparing the measured data with the calculated data, it appears that only 4.6% of the recombined ions were captured by the detector.

V. SUMMARY

Recombination signals have been successfully used for aligning the energy of the electrons with that of the ions in the CeC experiment during RHIC run 21, 22 and 25. Traditional electron cooling has been observed as a result of beam energy alignment. For beam parameters of the CeC experiment, the measured data can only be explained by a formalism which includes the effects from the transverse motion of the particles, i.e. the transverse angular spread and the orbital angles of the two beams in the cooling section. In this work, we have derived such formulism and used it to analyze the measured data collected during the CeC experiment. The results of our analysis yield reasonable estimates of the orbital alignment of the two beams in the cooling section, showing 50% reduction of the orbital angle after the beam-based alignments were performed.

ACKNOWLEDGMENTS

Work supported by Brookhaven Science Associates, LLC under Contract No. DE-SC0012704 with the U.S. Department of Energy.

[1] S. Seletskiy et al., Physical Review Accelerators and Beams 22, 111004 (2019).

[2] F. Carlier, M. Blaskiewicz, A. Drees, A. Fedotov, W. Fischer, M. Minty, C. Montag, G. Robert-Demolaize, and P. Thieberger, in the 7th International Particle Accelerator Conference (Busan, Korea, 2016), pp. 1239

[3] V. N. Litvinenko, in the 10th International Particle Accelerator Conference (Melbourne, Australia, 2019), p. 2101.

[4] G. Wang, arXiv: 2109.13980 (2021).

* gawang@bnl.gov